HHS Public Access

Author manuscript

Eur Radiol. Author manuscript; available in PMC 2022 March 01.

Published in final edited form as:

Eur Radiol. 2021 March ; 31(3): 1336–1346. doi:10.1007/s00330-020-07214-9.

T1, T2 MR Fingerprinting Measurements of Prostate Cancer and Prostatitis Correlate with Deep Learning Derived Estimates of Epithelium, Lumen and Stromal Composition on Corresponding Whole Mount Histopathology

Rakesh Shiradkar, PhD[1], **Ananya Panda, MD**[2,3], **Patrick Leo, BS**[1], **Andrew Janowczyk, PhD**[1], **Xavier Farre, MD**[4], **Nafiseh Janaki, MD**[5,6], **Lin Li, MS**[1], **Shivani Pahwa, MD**[3], **Amr Mahran, MD**[7], **Christina Buzzy, PhD**[7], **Ping Fu, PhD**[8], **Robin Elliott, PhD**[5], **Gregory MacLennan, MD**[5], **Lee Ponsky, MD**[7], **Vikas Gulani, MD, PhD**[3,9], **Anant Madabhushi, PhD**[1]

[1]Department of Biomedical Engineering, Case Western Reserve University, Cleveland, OH

[2]Department of Radiology, Mayo Clinic, Rochester, MN, USA

[3]Department of Radiology, University Hospitals, Cleveland, OH, USA

[4]Department of Public Health, Public Health Agency of Catalonia, Lleida, Catalonia, Spain

[5]Department of Pathology, University Hospitals, Cleveland, OH, USA

[6]Department of Pathology, Harvard Medical School, Brigham and Women's Hospital, Boston, MA, USA

Corresponding Author: Rakesh Shiradkar, PhD, rxs558@case.edu, *Telephone:* +1 216-368-3502, *Address*: Department of Biomedical Engineering (Wickenden 525), Case Western Reserve University, 10900 Euclid Avenue, Cleveland OH 44106, United States of America.

1. Guarantor:
The scientific guarantor of this publication is Dr. Anant Madabhushi.

2. Conflict of Interest:
The authors of this manuscript declare no relationships with any companies, whose products or services may be related to the subject matter of the article.

3. Statistics and Biometry:
Dr. Pingfu Fu kindly provided statistical advice for this manuscript.

4. Informed Consent:
Only if the study is on human subjects:
Written informed consent was provided by the patients for IRB protocol involving MRI and MRF acquisition. However, their consent was waived by the IRB for this specific study since it is retrospective and computational and poses very minimal risk to patients.

5. Ethical Approval:
Institutional Review Board approval was obtained.

6. Study subjects or cohorts overlap:
Some study subjects or cohorts have been previously reported in Yu et. al. *Radiology* 2017 which is attached with the manuscript.

7. Methodology
Methodology:
• retrospective
• observational / experimental
• performed at one institution

[7]Department of Urology, University Hospitals Cleveland, OH, USA

[8]Department of Population and Quantitative Health Sciences, School of Medicine, Case Western Reserve University, Cleveland, OH, USA

[9]Department of Radiology, University of Michigan, Ann Arbor, MI, USA

Abstract

Objectives—To explore associations between T1, T2 Magnetic Resonance Fingerprinting (MRF) measurements and corresponding tissue compartment ratios (TCRs) on whole mount histopathology of prostate cancer (PCa) and prostatitis.

Materials and Methods—A retrospective, IRB approved, HIPAA compliant cohort consisting of 14 PCa patients who underwent 3T multi-parametric MRI along with T1, T2 MRF maps prior to radical prostatectomy was used. Correspondences between whole mount specimens and MRI, MRF were manually established. Prostatitis, PCa and normal peripheral zone (PZ) regions of interest (ROIs) on pathology were segmented for TCRs of epithelium, lumen, and stroma using two U-net deep learning models. Corresponding ROIs were mapped to T2-weighted MRI(T2w), apparent diffusion coefficient(ADC), T1 and T2 MRF maps. Their correlations with TCRs were computed using Pearson's correlation coefficient (R). Statistically significant differences in means were assessed using one-way ANOVA.

Results—Statistically significant differences (p<0.01) in means of TCRs, T1, T2 MRF were observed between PCa, prostatitis and normal PZ. A negative correlation was observed between T1, T2 MRF and epithelium (R=−0.38, −0.44, p<0.05) of PCa. T1 MRF was correlated in opposite directions with stroma of PCa and prostatitis (R = 0.35, −0.44, p<0.05). T2 MRF was positively correlated with lumen of PCa and prostatitis (R=0.57, 0.46, p<0.01). Mean T2 MRF showed significant differences (p<0.01) between PCa and prostatitis across both transition zone (TZ) and PZ while mean T1 MRF was significant (p=0.02) in TZ.

Conclusion—Significant associations between MRF (T1 in the TZ and T2 in the PZ) and tissue compartments on corresponding histopathology were observed.

Keywords

Prostatic Neoplasms; Prostatitis; magnetic resonance imaging; Prostatectomy; Deep Learning

Introduction

Magnetic resonance fingerprinting (MRF) yields simultaneous and co-registered quantitative T1 and T2 maps [1]. In MRF, the MR system parameters are allowed to vary in a pseudorandom manner such that unique signal time-courses are produced for each combination of tissue properties of interest. The time course in each pixel is matched to a dictionary consisting of all possible ranges of signal evolutions, yielding the properties of interest for each pixel [1].

Yu et. al. [2] have shown T1, T2 MRF along with echo-planar based apparent diffusion coefficient (ADC) maps could distinguish cancerous and normal prostate in the peripheral

zone with a near perfect separation. Panda et. al. have recently shown that these measurements were significantly different between prostate cancer and prostatitis in the peripheral[3] and transition zone[4], and show excellent diagnostic performance in differentiating prostate cancer and non-cancer. However, a morphologic basis of MRF is important to understand pathologic attributes driving the T1, T2 measurements [5].

Correlation of histopathology and MR imaging is vital for gaining deeper insights into the characterization of prostate cancer on imaging. Previous studies [6–8] have explored correlations between prostate multi-parametric MRI (mpMRI) and digitized histopathology [7, 8]. Associations between ADC derived from diffusion weighted imaging (DWI) [8–11], between T2-weighted (T2w) [8, 9], dynamic contrast enhanced (DCE) imaging parameters and tissue compartments including epithelium, lumen and stroma have also been studied. However, there has been no study evaluating the associations between both T1 and T2 relaxation times with paired histopathology.

Being able to differentiate non-cancers from cancers may significantly improve characterization of prostate cancer on imaging. While a few previous studies have shown that mpMRI could potentially help in differentiating prostatitis and prostate cancer [12–14], overlapping characteristics still exist on imaging [15–18]. Quantitative MRF can potentially help in addressing these challenges as evidenced in recently published works [3, 4]. However, there is a need to evaluate the interpretability of these findings, specifically with respect to corresponding histopathologic characteristics. Establishing a histo-morphometric basis of MRF measurements for prostate cancer diagnosis would improve clinical adoption of MRF and also potentially improve MRF acquisition. The rationale of this paper is to explore and establish the histo-morphometric basis for MRF-based T1 and T2 relaxometry measurements that have previously been shown to be strongly associated with prostate cancer. These results could potentially help future studies on refining MRF acquisition and aid in improving characterization of prostate cancer on imaging. To our knowledge, none of the previous studies have explored differential correlations between quantitative T1, T2 maps and histopathology with respect to prostate cancer and prostatitis.

In this study, our goal is to establish a histo-morphometric basis that drive MRF-relaxometry measurements for characterizing prostate cancer and prostatitis. We correlate histologic parameters from deep learning based segmentations of tissue compartments on prostate whole mount pathology with corresponding T1, T2 MRF maps. We explore these associations within prostate cancer, prostatitis and normal peripheral zone (NPZ) regions of interest (ROIs) delineated on pathology which are then mapped back on to corresponding MRI and MRF via deformable co-registration. Since imaging characteristics of lesions within the peripheral (PZ) and transition zone (TZ) on imaging are different[19], we also explore the differences in associations between the zones as well.

Materials and Methods

This retrospective study was approved by the local institutional review board (IRB), is Health Insurance Portability and Accountability Act (HIPAA) compliant and used anonymized data stripped of any protected health information. From February 2014 to April

2016, 133 patients (after informed consent for MRI with MRF) with suspicion of prostate cancer underwent MR imaging with MR Fingerprinting on a 3T MRI scanner (Skyra, Siemens, Erlangen, Germany) before 12-core trans-rectal ultrasound guided biopsy with/without cognitive targeting. These patients were part of a previously published study [2] of which N = 19 patients who underwent radical prostatectomy (RP) were identified and included in this study. Patients with reconstruction artifacts, discordant pathology findings including non-visible lesions on MRI, distorted whole mount slides, or scanning artifacts were excluded and finally N = 14 patients were included in this study (Figure 1). The median time difference between imaging and surgery was 3 months (range 0 – 14 months).

MRI, MRF protocol

Multi-parametric MRI protocol included acquisition of T2w (resolution: 0.6 × 0.6 mm., slice thickness: 3 mm., TR/TE: 8600/103 ms., duration: 3.3 min.), DWI (resolution: 1.2 × 1.2 mm., slice thickness: 3 mm., TR/TE: 7900/88 ms., *b*-values: 50 – 1400 s/mm^2, duration: 4.46 min.) along with ADC maps via pelvicphased array coil (Skyra, Siemens). Dynamic contrast enhanced (DCE) was acquired but not used in this study. MRF was acquired by fast imaging with steady-state precision [1] and quantitative T1 and T2 maps (resolution: 1.0 × 1.0 mm., slice thickness: 5 mm., TR/TE: 13 – 15 ms., duration: 0.39 min. per slice) were generated via software (MATLAB v.20xx, MathWorks Inc.), as detailed in previous work [2]. The total acquisition time was about 40 minutes (including mpMRI and MRF). Details of clinical parameters are provided in Table 1 and imaging parameters are summarized in the supplementary material (Table S1).

T2w images were corrected for intensity drift related artifacts using a previously presented method [20] that aligns histograms of voxel intensities, such that resultant intensities have a tissue specific meaning. To enable alignment of ROIs, ADC maps were linearly interpolated and up sampled to match the resolution of T2w. The linear interpolation affected the resultant ADC values by <0.02 % and did not introduce any significant differences.

Digitized histopathology, annotations, and tissue compartment segmentation

Post-surgical prostate specimens were sliced at 5mm thickness and stained with hematoxylin and eosin (H&E) for microscopic evaluation. Each slice was then digitized using a standard brightfield optical microscope (Aperio Technologies) at a resolution of 20×. An experienced pathologist delineated regions of interest (ROI) including prostate cancer, prostatitis and normal peripheral zone (NPZ) on digitized whole mount (WM) sections using software (Aperio ImageScope v12.0). The ROIs for PCa were drawn such that at least 90% of the ROI was cancerous without benign/normal tissue. Chronic prostatitis was considered in this study which is characterized by contiguous gland spaces meeting consecutive inflamed glands with intra luminal neutrophils and intervening stromal lymphocytes. Since majority of PCa lesions originate in the PZ, and most patients in the cohort being elderly, there was significant benign prostatic hyperplasia resulting in a heterogeneous appearance of transition zone. Therefore, normal prostate ROIs were identified within the peripheral zone. ROIs with radius along the shortest axis < 3 mm were discarded as such small isolated lesions at the micron scale could not be discerned at the MR scale.

Tissue compartment segmentation involved identifying regions of epithelium, lumen, and stroma within the ROI's on WM. For this, two different U-net based deep learning models were used – the first model was an epithelium-stroma segmentation model and the second was a lumen segmentation model. Separate U-net segmentation models[21] were trained since the first model used images at higher resolution (20×) than the second (5×). Segmentation of three tissue compartments was achieved combining the result from two different models. The tissue compartment segmentations were reviewed by the pathologist to confirm the accuracy of segmentations. Additional details with respect to the training and validation of these deep learning models are provided in the supplemental section.

For each ROI on WM, segmentations obtained from the two deep learning models were integrated to generate tissue compartment maps. For pixels which were predicted positive by both models, the lumen class was given precedence due to its relatively higher TPR (an example is illustrated in Figure 2a). These maps were subsequently employed to estimate tissue compartment ratios (TCRs) for epithelium, lumen, and stroma within the ROIs.

Registration between histopathology, MRI and MRF

An experienced radiologist (>9 years of experience in genitourinary radiology) and pathologist (with >10 years of experience in prostate pathology) together identified the best possible set of corresponding slices between T2w images and digitized WM. The mid-gland region was considered for correspondence since intact WM at the apex and base were not always available. Since the spacing and alignment of T2w images and WM slices may not be coincide in all studies, a visual approach based on landmarks (urethra, presence of nodules, peripheral zone, cancerous lesion) was adopted to determine the closest match. The correspondence between MRI and MRF is straightforward and was determined by the radiologist.

The ROIs corresponding to PCa, prostatitis and NPZ were delineated by the pathologist on WM. These ROIs were mapped on to MRI and MRF via a 2-step registration process. Once the slice correspondences between MR and histopathology were established, a deformable registration was performed to align WM with T2w images. The mean dice similarity coefficient (DSC) measuring the overlap of prostate boundary (delineated by the radiologist) on T2w and pathology was 0.85 and the mean target registration error was 1.2 mm, indicating a reasonably good mapping. The T2w and ADC were co-registered via a rigid transformation and the ROI on T2w was mapped on to ADC. The ROIs on T2w and ADC were verified by the radiologist and slightly adjusted if the ROI was not aligned with corresponding suspicious region on MRI. Next, T2w and T2 MRF were aligned using another deformable registration and using this learned transformation, the ROI from T2w was mapped on to T2 MRF. ROIs were only mapped on T2 MRF maps, as these are implicitly co-registered with T1 MRF maps and both T1 and T2 information can be obtained simultaneously. All registrations were performed using a previously presented method [22] that was implemented using the software Elastix [23].

Statistical Analysis

The distribution of imaging variables (T1, T2 MRF, ADC, T2w MRI) and TCRs within the ROIs follow a continuous distribution. Therefore, to estimate the linear relationship between MR measurements and TCRs, Pearson's correlation coefficient (R) was computed. On the other hand, the International Society of Urologic Pathology Prognostic Groups (IPG) is an ordinal variable and therefore, the Spearman's rank correlation (ρ) was used compute the monotonic relationship between IPG and each of the imaging variables, TCRs. The differences between mean MRI, MRF measurements, tissue compartments across IPGs, prostatitis and NPZ ROIs was examined using one-way analysis of variance (ANOVA) test followed by multiple pair-wise comparisons using Tukey honest significant differences (HSD) post-hoc test. Simple pair-wise comparisons were performed using the Wilcoxon rank-sum test with $p < 0.05$ considered to be statistically significant. This is a non-parametric test that assesses whether the distributions between two separate groups are statistically significant. Statistical analyses were performed in MATLAB (v.2018a, MathWorks Inc.) and R [24]. The ROIs obtained on MRI via mapping were eroded by 3 voxels (= 1.8 mm.) on MRI, and 2 voxels (= 2mm.) on MRF, to discard any noise arising from artifacts at the boundary of ROIs.

Mean T1, T2 MRF and ADC were all statistically significant univariate predictors of PCa (N = 33 lesions) compared to NPZ (N = 24 ROIs). A multi-variable logistic regression model with T1, T2 MRF and ADC together resulted in AUC = 0.997 in distinguishing PCa and NPZ. These observations are in line with previously published study by Yu et. al. [2], who reported AUC = 0.99 in distinguishing PCa from NPZ with N = 109 lesions using T1, T2 MRF and ADC together. Patients in this study are a subset of those reported in the study by Yu et. al.

Results

Associations between MRF, tissue compartments, and IPG

From the set of $N = 14$ patients, 33 cancerous, 23 prostatitis and 24 NPZ ROIs were identified on histopathology and mapped on to MRI and MRF. Distribution of lesions belonging to various ISUP Prognostic Groups (IPG) are summarized in Table 1. The tissue compartment estimates within PCa, prostatitis and NPZ ROIs along with mean T1, T2 MRF measurements, ADC values, and T2w intensities are summarized in Table 2. All these measurements were observed to be statistically significant ($p < 0.001$) across IPGs, prostatitis and NPZ on ANOVA. Multiple pair-wise comparisons are detailed in Supplementary Table S2 which show that T1, T2 MRF and ADC measurement were significantly different ($p < 0.05$) between PCa (across all IPGs) and NPZ.

Density of epithelium was observed to increase with IPG ($\rho = 0.89$) while that of lumen and stroma decreased with IPG ($\rho = -0.71$ and -0.73). Tissue compartment ratios (TCR) of epithelium and stroma in prostatitis were found to be similar to clinically insignificant PCa (IPG = 1), however, were significantly different compared to NPZ ($p < 0.05$). MRF T2 and ADC dropped ($R = -0.39$ and -0.56) with increasing IPG within the PCa ROIs. MRF T2 and ADC in prostatitis ROIs were observed to be higher than all PCa (including IPG = 1).

T1 MRF measurements also followed a similar trend as T2 MRF, ADC however a statistical significance was not observed. All of T1, T2 MRF and ADC measurements were significantly higher in NPZ compared to PCa and prostatitis (Figure 4).

Correlations between MRF and tissue compartments within prostate cancer and prostatitis ROIs

Significant correlations between TCRs and MRF measurements on imaging were observed (Figure 3). T1 MRF was positively correlated with stroma for PCa ($R = 0.35$) and negatively correlated for prostatitis ($R = -0.44$). T1 MRF was negatively correlated with epithelium for PCa ($R = -0.38$) while no significant correlations were observed in prostatitis and with lumen TCRs. There was a negative correlation of T2 MRF measurements with density of epithelium ($R = -0.44$) and positive correlation with lumen ($R = 0.57$) for prostate cancer. While T2 MRF was also positively correlated with lumen for prostatitis ($R = 0.46$), no significant association was observed with epithelium in this case. ADC measurements were negatively correlated to epithelial TCR and positively correlated to TCRs stroma and lumen within the cancerous ROIs. However, no significant associations were observed for prostatitis (provided in supplemental section).

Correlations between T1 MRF and stromal ratio were found to be in opposite directions for prostate cancer and prostatitis (Figure 3). Significant differences ($p < 0.01$) were observed in T2 MRF and ADC measurements between prostate cancer and prostatitis in both the peripheral zone (PZ) and the transition zone (TZ) (Figure 4). T1 MRF measurements showed significant differences between these two categories in the TZ.

Differences in MRF – tissue compartment associations in peripheral and transition zone prostate cancer lesions

When controlled for their location in specific zones, stronger correlations between T2 MRF, ADC and TCRs was observed within the PZ PCa lesions while T1 MRF showed higher correlations with epithelium and stromal ratio within the TZ lesions. ADC was found to be strongly correlated to the lumen ration within TZ PCa lesions. These results are summarized in Table 3. With respect to prostatitis, significant correlations between TCRs and T1, T2 MRF were observed in the TZ while no significant correlations were observed in the PZ.

Discussion

The goal of this study was to establish associations between ground truth histopathology and corresponding MRF measurements which could help facilitate a better understanding and interpretability of the morphologic basis of the MRF parameters and potentially optimize MRF acquisition towards discriminating specific pathologic presentations. In this study, we explored associations between T1, T2 MRF and tissue compartment ratios (TCRs) within regions of prostate cancer (PCa), prostatitis and normal peripheral zone (NPZ). A carefully curated cohort of patients who underwent radical prostatectomy (RP) prior to MR examination was used and whole mount sections of prostate post RP were co-registered with *in vivo* MRI and MRF. The co-registration was used to define delineations of prostate cancer (PCa), prostatitis and NPZ regions of interest (ROIs) on imaging, verified by an experienced

radiologist and pathologist. Deep learning derived tissue compartment ratios (TCRs) of epithelium, lumen, and stroma on histopathology were correlated with T1, T2 measurements within corresponding ROIs on MRF.

Previous studies have investigated diagnostic performance of MRF and have shown that T1, T2 and ADC measurements resulted in excellent separation between cancers and non-cancers. Yu et. al. [2] have shown that T1, T2 MRF and ADC separated PCa from normal prostate in the peripheral zone (PZ) with an AUC=0.99 on a dataset of N=109 lesions. Panda et. al.[3] further explored and found that T1 and ADC together resulted in AUC=0.83 in distinguishing PCa and prostatitis on a set of N=104 lesions in the PZ. In a separate study, Panda et. al. [4] investigated N=75 lesions in the transition zone (TZ) and observed that T1 and ADC together resulted in an AUC=0.94 in separating cancers from non-cancers.

In this study, correlations assessed between MRF measurements and ISUP Prognostic Groups (IPG) revealed that T2 MRF and ADC dropped with increasing IPG which is consistent with previous results [7, 25, 26]. The epithelium ratio is significantly higher and lumen ratio significantly lower in high grade lesions (IPG = 4,5) which results in restricted diffusion in lumen and is reflected in reduction of T2 relaxation time and ADC [27]. Measurements of T1, T2 MRF and ADC were significantly different between PCa and NPZ on ANOVA followed by multiple pair-wise comparisons. This indicates that healthy prostate tissue has significantly higher measurements compared to PCa and prostatitis. These are also illustrated in Figure 5. Mean T2 MRF and ADC were lower in cancer ROIs (including low grade IPG = 1) compared to prostatitis which has also been shown in previous studies by Panda et. al. [3, 4]. Prostatitis is characterized by the presence of lymphocytes in stroma and intra-luminal neutrophils [28] which also tends to result in restriction of diffusion, however this is lesser than that observed in PCa. These observations have been reported by earlier studies [12, 29] and our results are in agreement.

Within PCa ROIs, we observed that T2 MRF measurements decreased with rise in epithelium and decline of lumen, which is in line with previously published literature [8, 11, 27]. T2 values are affected by free water and fluid [30] in the extracellular space which is significantly reduced in PCa due to a high epithelial content and poorly formed glands. T1 MRF measurements decreased with rise in epithelium and reduction of stroma compared to healthy prostate tissue as illustrated in Figure 5. The breakdown of glandular spaces that contain fluid results in shorter T1 and this was also observed in a study by Busch et.al. [31] which looked at T1 relaxation in *ex vivo* prostate tissue. We also computed correlations between conventional MRI (T2w, ADC maps) and TCRs and our results were in agreement with previous studies for PCa lesions, as shown in Table 4. Kwak et. al. (16) used the Pearson's correlation coefficient as used in our study and our results are in close agreement. This provides a sanity check that despite differences in datasets and methods used to segment tissue compartments, the correlations between prostate cancer MRI and pathology remain similar.

For prostatitis, T2 MRF measurements reduced with decrease in lumen TCRs, similar to what was observed for PCa. However, on histopathology, while prostatitis is characterized by intraluminal neutrophils and glandular atrophy [32] PCa shows decreased luminal

volume. We also observed that lower stromal TCR was associated with higher T1 MRF. In our segmentation approach, lymphocytes were not categorized separately and regions with a high concentration of infiltrating lymphocytes were segmented as epithelium. Therefore, a lower stromal content could imply a higher concentration of lymphocytes, or inflammatory cells, along with extracellular fluid in the *in vivo* tissue [14]. Taken together, this would result in a higher T1 signal. However, further studies on a larger dataset are needed to gain additional insights.

Significant differences between prostatitis and PCa have been observed in our study with respect to ADC and T2 MRF. When individual prostate zones were considered, ADC and T2 MRF measurements were significantly different both in the peripheral (PZ) and transition zone (TZ), while T1 MRF was significantly different in the TZ. These results are in agreement with some of the recent studies by Panda et. al. [3, 4] which demonstrated that T1, T2 MRF and ADC were significantly different between prostatitis and PCa. Results using quantitative MRF measurements and ADC tend to indicate that they could potentially be capturing morphologic differences between prostate cancer and prostatitis. Validation on a larger cohort of patient studies will be conducted in the future to establish these findings.

When controlling for the spatial location of the disease, we observed correlations between T1 MRF and TCRs were stronger and significant in the TZ (both PCa and prostatitis) while those between T2 MRF and TCRs were stronger in the PZ. A number of earlier studies including the Prostate Imaging Reporting and Data System version 2 (PIRADS v2) guidelines [33], and radiomic signatures derived from MRI [19, 34] indicated that PZ and TZ tumors tend to have different characteristics and this observation also held with respect to MRF measurements.

Our study did have its limitations. The number of patients used in this study were limited and from a single institution which may affect the robustness and generalizability of these findings. Nevertheless, a majority of observations were in line with previous studies. Future work will include validating these findings on a larger cohort across multiple scanners, institutions and perform multiple comparisons. Co-registration of MRI, MRF and pathology was based on slice correspondences that were manually established by a single radiologist and pathologist which may be potentially biased. However, characteristics of cancer tissue on pathology are well defined and ROIs on pathology were defined to contain > 90% of cancerous tissue. Therefore, we anticipate a very minimal error rate on account of inter-reader variations in this study. One of the possible ways to minimize this error in the future is to employ an *in vivo* imaging based mold for sectioning of whole mounts post-surgery[6] and this is a part of our ongoing study. In this study, we have considered individual lesions separately and there might be correlations between lesions from the same patient. However, due consideration has been given such that clusters of lesion on pathology which would appear as a single, continuous hypo-intense region on imaging were matched accordingly. Segmentation of tissue compartments on pathology was limited to epithelium, lumen & stroma and future work could include more detailed annotations [35], radiomic feature characterization on pathology and training of sub-compartment models including lymphocyte concentration, cytoplasm, macrophages to better characterize benign lesions.

In conclusion, we observed significant correlations between tissue compartments on pathology and T1, T2 MRF maps. Increase in epithelial density with IPG was reflected in lower T2 MRF measurements and an inverse relationship was observed with respect to density of lumen. Reduction in stromal content with rise in IPG was captured by T1 MRF measurements. T2 MRF measurements showed differences between prostate cancer and prostatitis and these trends were also observed with low grade prostate cancer and prostatitis. The understanding gained in this study, of the histo-morphometric basis for differences in T1 and T2 relaxation times (as seen on MRF) between normal peripheral zone, prostatitis and cancerous tissue, could play an important role in helping design strategies for future MRF acquisitions. For instance, T1 and T2 MRF measurements could be combined with other MR measurements, considering their differential correlations with tissue compartments, that may further emphasize these tissue differences.

Supplementary Material

Refer to Web version on PubMed Central for supplementary material.

Acknowledgements and funding:

Research reported in this manuscript was supported by the National Cancer Institute of the National Institutes of Health under award numbers 1U24CA199374–01, R01CA202752–01A1, R01CA208236–01A1, R01 CA216579–01A1, R01 CA220581–01A1, 1U01 CA239055–01 National Center for Research Resources under award number 1 C06 RR12463–01 VA Merit Review Award IBX004121A from the United States Department of Veterans Affairs Biomedical Laboratory Research and Development Service the DOD Prostate Cancer Idea Development Award (W81XWH-15–1-0558) the DOD Lung Cancer Investigator-Initiated Translational Research Award (W81XWH-18–1-0440) the DOD Peer Reviewed Cancer Research Program (W81XWH-16–1-0329) the Ohio Third Frontier Technology Validation Fund the Wallace H. Coulter Foundation Program in the Department of Biomedical Engineering and the Clinical and Translational Science Award Program (CTSA) at Case Western Reserve University. The DoD Prostate Cancer Research Program Idea Development Award W81XWH-18–1-0524

Abbreviations

ADC	Apparent Diffusion Coefficient
ANOVA	Analysis of Variance
IPG	International Society of Urologic Pathology (ISUP) Prognostic Groups
MRF	Magnetic Resonance Fingerprinting
NPZ	Normal Peripheral Zone
PCa	Prostate Cancer
PZ	Peripheral Zone
T2w	T2-weighted
TCR	Tissue Compartment Ratio
TZ	Transition Zone
WM	Whole Mount Histopathology

References

1. Ma D, Gulani V, Seiberlich N, et al. (2013) Magnetic resonance fingerprinting. Nature 495:187–192. 10.1038/nature11971 [PubMed: 23486058]
2. Yu AC, Badve C, Ponsky LE, et al. (2017) Development of a Combined MR Fingerprinting and Diffusion Examination for Prostate Cancer. Radiology 283:729–738. 10.1148/radiol.2017161599 [PubMed: 28187264]
3. Panda A, O'Connor G, Lo WC, et al. (2019) Targeted Biopsy Validation of Peripheral Zone Prostate Cancer Characterization With Magnetic Resonance Fingerprinting and Diffusion Mapping. Invest Radiol 10.1097/RLI.0000000000000569
4. Panda A, Obmann VC, Lo W-C, et al. (2019) MR Fingerprinting and ADC Mapping for Characterization of Lesions in the Transition Zone of the Prostate Gland. Radiology 181705 10.1148/radiol.2019181705
5. Penzias G, Singanamalli A, Elliott R, et al. (2018) Identifying the morphologic basis for radiomic features in distinguishing different Gleason grades of prostate cancer on MRI: Preliminary findings. PloS One 13:e0200730 10.1371/journal.pone.0200730 [PubMed: 30169514]
6. Turkbey B, Mani H, Shah V, et al. (2011) Multiparametric 3T prostate magnetic resonance imaging to detect cancer: histopathological correlation using prostatectomy specimens processed in customized magnetic resonance imaging based molds. J Urol 186:1818–1824. 10.1016/j.juro.2011.07.013 [PubMed: 21944089]
7. Chatterjee A, Watson G, Myint E, et al. (2015) Changes in Epithelium, Stroma, and Lumen Space Correlate More Strongly with Gleason Pattern and Are Stronger Predictors of Prostate ADC Changes than Cellularity Metrics. Radiology 277:751–762. 10.1148/radiol.2015142414 [PubMed: 26110669]
8. Kwak JT, Sankineni S, Xu S, et al. (2017) Prostate Cancer: A Correlative Study of Multiparametric MR Imaging and Digital Histopathology. Radiology 285:147–156. 10.1148/radiol.2017160906 [PubMed: 28582632]
9. Langer DL, van der Kwast TH, Evans AJ, et al. (2010) Prostate tissue composition and MR measurements: investigating the relationships between ADC, T2, K(trans), v(e), and corresponding histologic features. Radiology 255:485–494. 10.1148/radiol.10091343 [PubMed: 20413761]
10. Gibbs P, Liney GP, Pickles MD, et al. (2009) Correlation of ADC and T2 measurements with cell density in prostate cancer at 3.0 Tesla. Invest Radiol 44:572–576. 10.1097/RLI.0b013e3181b4c10e [PubMed: 19692841]
11. Chatterjee A, Bourne RM, Wang S, et al. (2018) Diagnosis of Prostate Cancer with Noninvasive Estimation of Prostate Tissue Composition by Using Hybrid Multidimensional MR Imaging: A Feasibility Study. Radiology 287:864–873. 10.1148/radiol.2018171130 [PubMed: 29393821]
12. Nagel KNA, Schouten MG, Hambrock T, et al. (2013) Differentiation of prostatitis and prostate cancer by using diffusion-weighted MR imaging and MR-guided biopsy at 3 T. Radiology 267:164–172. 10.1148/radiol.12111683 [PubMed: 23329653]
13. Esen M, Onur MR, Akpolat N, et al. (2013) Utility of ADC measurement on diffusion-weighted MRI in differentiation of prostate cancer, normal prostate and prostatitis. Quant Imaging Med Surg 3:210–216. 10.3978/j.issn.2223-4292.2013.08.06 [PubMed: 24040617]
14. Sah VK, Wang L, Min X, et al. (2015) Multiparametric MR imaging in diagnosis of chronic prostatitis and its differentiation from prostate cancer. Radiol Infect Dis 1:70–77. 10.1016/j.jrid.2015.02.004
15. Rosenkrantz AB, Taneja SS (2014) Radiologist, be aware: ten pitfalls that confound the interpretation of multiparametric prostate MRI. AJR Am J Roentgenol 202:109–120. 10.2214/AJR.13.10699 [PubMed: 24370135]
16. Dianat SS, Carter HB, Pienta KJ, et al. (2015) Magnetic resonance-invisible versus magnetic resonance-visible prostate cancer in active surveillance: a preliminary report on disease outcomes. Urology 85:147–153. 10.1016/j.urology.2014.06.085 [PubMed: 25440986]
17. Marks LS (2016) Some prostate cancers are invisible to magnetic resonance imaging! BJU Int 118:492–493. 10.1111/bju.13440 [PubMed: 27625328]

18. Yu J, Fulcher AS, Turner MA, et al. (2014) Prostate cancer and its mimics at multiparametric prostate MRI. Br J Radiol 87:20130659 10.1259/bjr.20130659 [PubMed: 24646125]
19. Viswanath SE, Bloch NB, Chappelow JC, et al. (2012) Central gland and peripheral zone prostate tumors have significantly different quantitative imaging signatures on 3 Tesla endorectal, in vivo T2-weighted MR imagery. J Magn Reson Imaging JMRI 36:213–224. 10.1002/jmri.23618 [PubMed: 22337003]
20. Nyúl LG, Udupa JK (1999) On standardizing the MR image intensity scale. Magn Reson Med 42:1072–1081 [PubMed: 10571928]
21. Ronneberger O, Fischer P, Brox T (2015) U-Net: Convolutional Networks for Biomedical Image Segmentation In: Navab N, Hornegger J, Wells WM, Frangi AF (eds) Medical Image Computing and Computer-Assisted Intervention – MICCAI 2015. Springer International Publishing, Cham, pp 234–241
22. Li L, Pahwa S, Penzias G, et al. (2017) Co-Registration of ex vivo Surgical Histopathology and in vivo T2 weighted MRI of the Prostate via multi-scale spectral embedding representation. Sci Rep 7:8717 10.1038/s41598-017-08969-w [PubMed: 28821786]
23. Klein S, Staring M, Murphy K, et al. (2010) elastix: a toolbox for intensity-based medical image registration. IEEE Trans Med Imaging 29:196–205. 10.1109/TMI.2009.2035616 [PubMed: 19923044]
24. R Core Team (2013) R: A Language and Environment for Statistical Computing. R Foundation for Statistical Computing, Vienna, Austria
25. Surov A, Meyer HJ, Wienke A (2019) Correlations between Apparent Diffusion Coefficient and Gleason Score in Prostate Cancer: A Systematic Review. Eur Urol Oncol. 10.1016/j.euo.2018.12.006
26. Hoang Dinh A, Souchon R, Melodelima C, et al. (2015) Characterization of prostate cancer using T2 mapping at 3T: a multi-scanner study. Diagn Interv Imaging 96:365–372. 10.1016/j.diii.2014.11.016 [PubMed: 25547670]
27. Langer DL, van der Kwast TH, Evans AJ, et al. (2008) Intermixed normal tissue within prostate cancer: effect on MR imaging measurements of apparent diffusion coefficient and T2--sparse versus dense cancers. Radiology 249:900–908. 10.1148/radiol.2493080236 [PubMed: 19011187]
28. Nickel JC, True LD, Krieger JN, et al. (2002) Consensus development of a histopathological classification system for chronic prostatic inflammation: HISTOLOGICAL CLASSIFICATION OF CHRONIC PROSTATITIS. BJU Int 87:797–805. 10.1046/j.1464-410x.2001.02193.x
29. Kitzing YX, Prando A, Varol C, et al. (2016) Benign Conditions That Mimic Prostate Carcinoma: MR Imaging Features with Histopathologic Correlation. Radiogr Rev Publ Radiol Soc N Am Inc 36:162–175. 10.1148/rg.2016150030
30. Mitchell DG, Burk DL, Vinitski S, Rifkin MD (1987) The biophysical basis of tissue contrast in extracranial MR imaging. AJR Am J Roentgenol 149:831–837. 10.2214/ajr.149.4.831 [PubMed: 3307357]
31. Busch S, Hatridge M, Mößle M, et al. (2012) Measurements of T1-relaxation in ex vivo prostate tissue at 132 μT. Magn Reson Med 67:1138–1145. 10.1002/mrm.24177 [PubMed: 22294500]
32. Kohnen PW, Drach GW (1979) Patterns of inflammation in prostatic hyperplasia: a histologic and bacteriologic study. J Urol 121:755–760. 10.1016/s0022-5347(17)56980-3 [PubMed: 88527]
33. Turkbey B, Choyke PL (2015) PIRADS 2.0: what is new? Diagn Interv Radiol Ank Turk 21:382–384. 10.5152/dir.2015.15099
34. Ginsburg SB, Algohary A, Pahwa S, et al. (2017) Radiomic features for prostate cancer detection on MRI differ between the transition and peripheral zones: Preliminary findings from a multi-institutional study. J Magn Reson Imaging JMRI 46:184–193. 10.1002/jmri.25562 [PubMed: 27990722]
35. Leo P, Elliott R, Shih NNC, et al. (2018) Stable and discriminating features are predictive of cancer presence and Gleason grade in radical prostatectomy specimens: a multi-site study. Sci Rep 8:14918 10.1038/s41598-018-33026-5 [PubMed: 30297720]

Key Points

1. Mean T2 MRF measurements and ADC within cancerous regions of interest dropped with increasing ISUP prognostic groups (IPG).
2. Mean T1 and T2 MRF measurements were significantly different ($p < 0.001$) across IPGs, prostatitis and normal peripheral zone (NPZ).
3. T2 MRF showed stronger correlations in peripheral zone while T1 MRF showed stronger correlations in the transition zone with histopathology for prostate cancer.

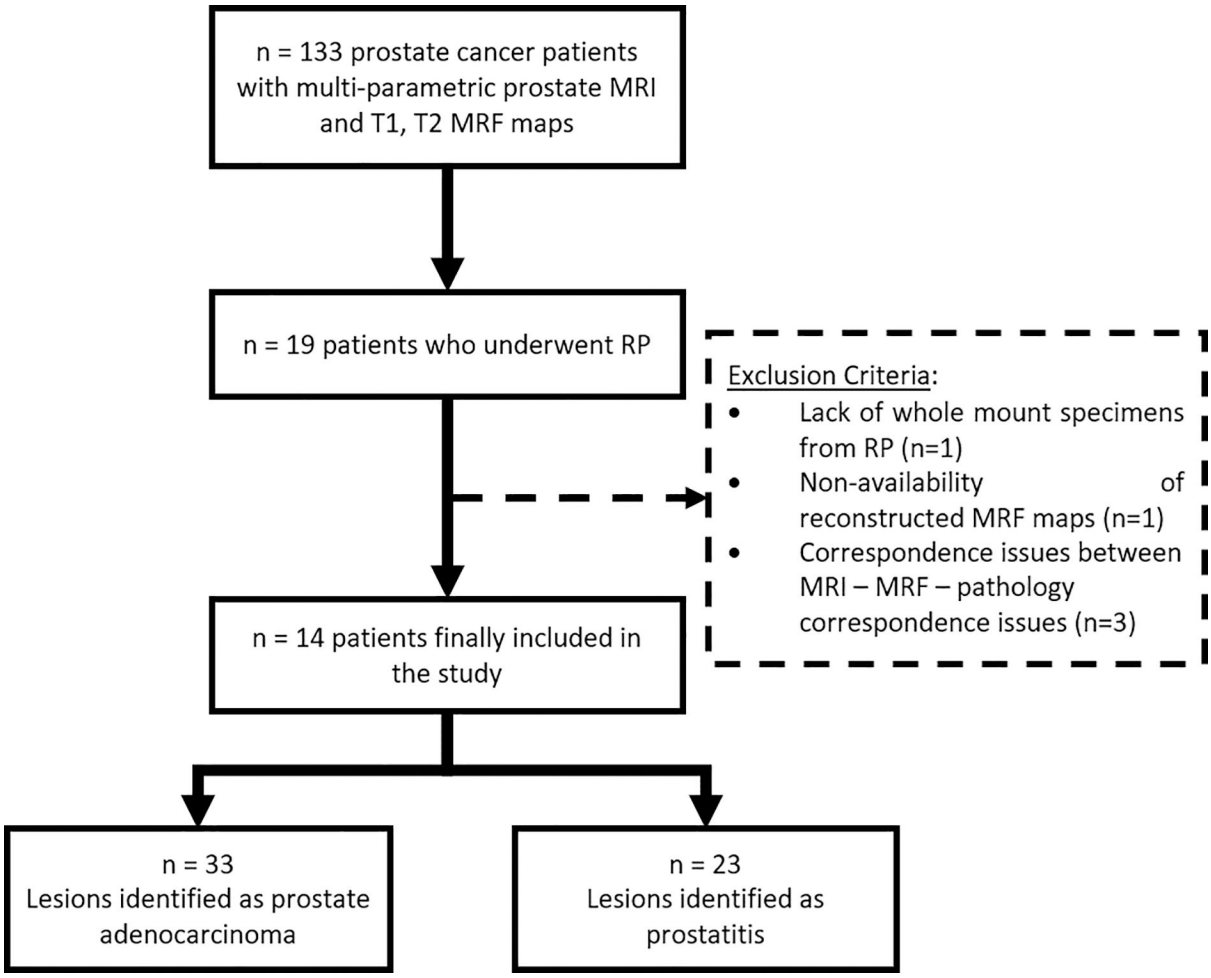

Figure 1:
Flowchart illustrating inclusion criteria for patients used in this study. RP: Radical prostatectomy, MRF: Magnetic Resonance Fingerprinting

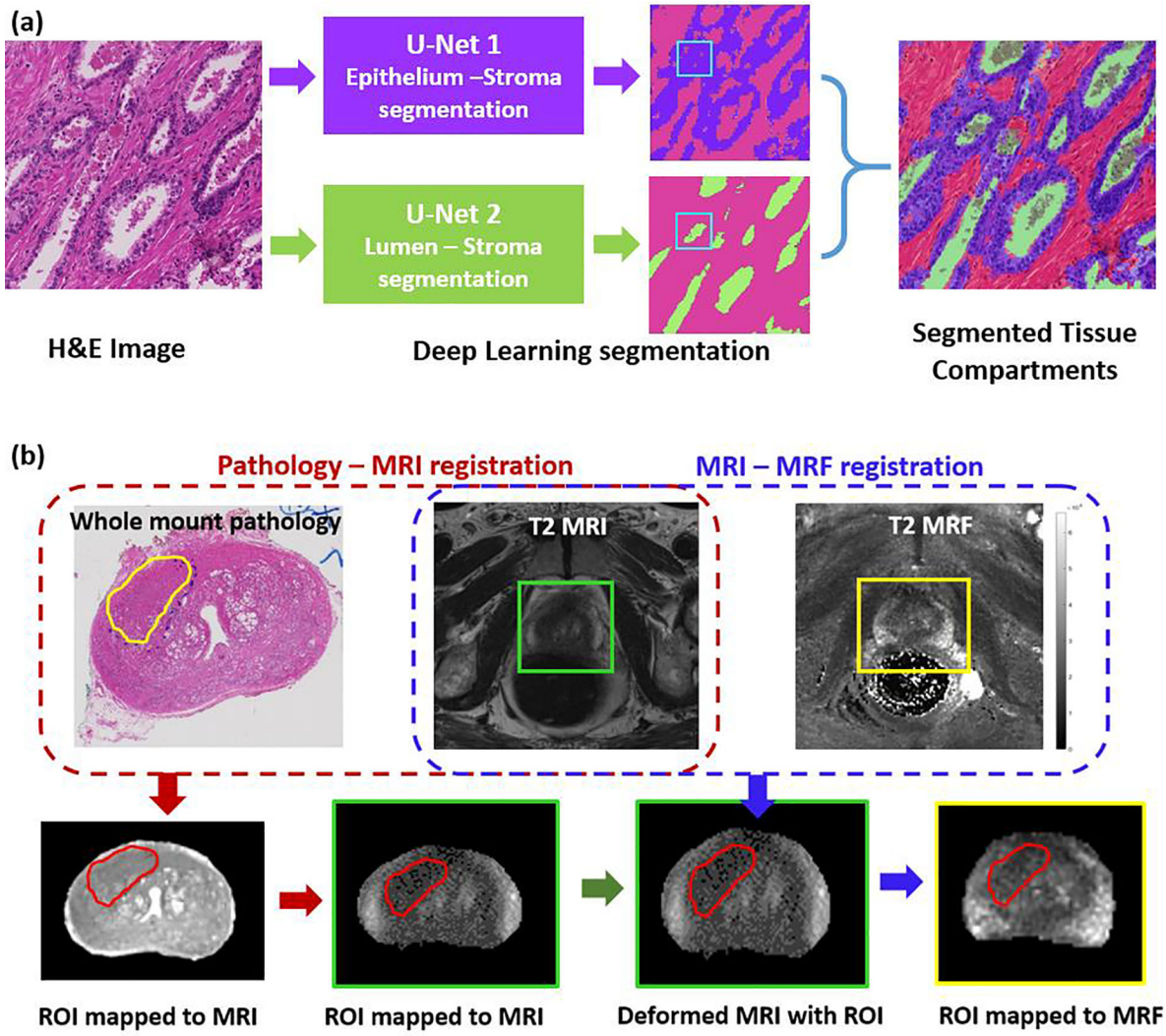

Figure 2:

(a) Tissue compartment segmentation on whole mount H&E stained digitized pathology using two U-net deep learning models. The lumen segmentation model has precedence when both the models are positive (an example is illustrated). (b) Schematic pipeline illustrating the workflow adopted to register digitized whole mounts with T2w images and T2 MRF. Prostate cancer and prostatitis ROIs delineated on pathology were mapped on to MRI and MRF following the registration.

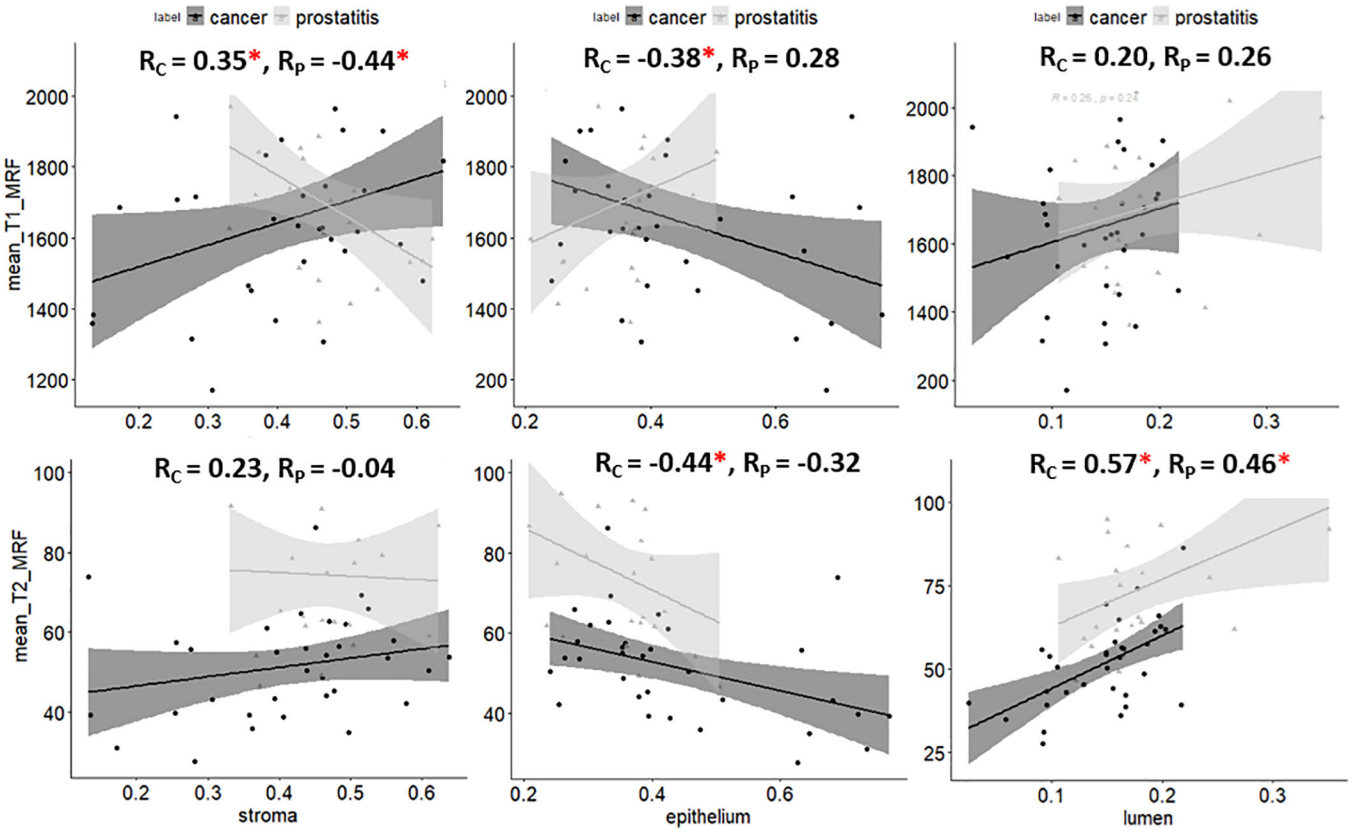

Figure 3:

Scatter plots of mean T1, T2 MRF with respect to tissue compartment ratios (TCRs) of stroma, epithelium and lumen within prostate cancer and prostatitis regions of interest. An asterisk is indicated next to correlation coefficient (*R*) to suggest statistical significance.

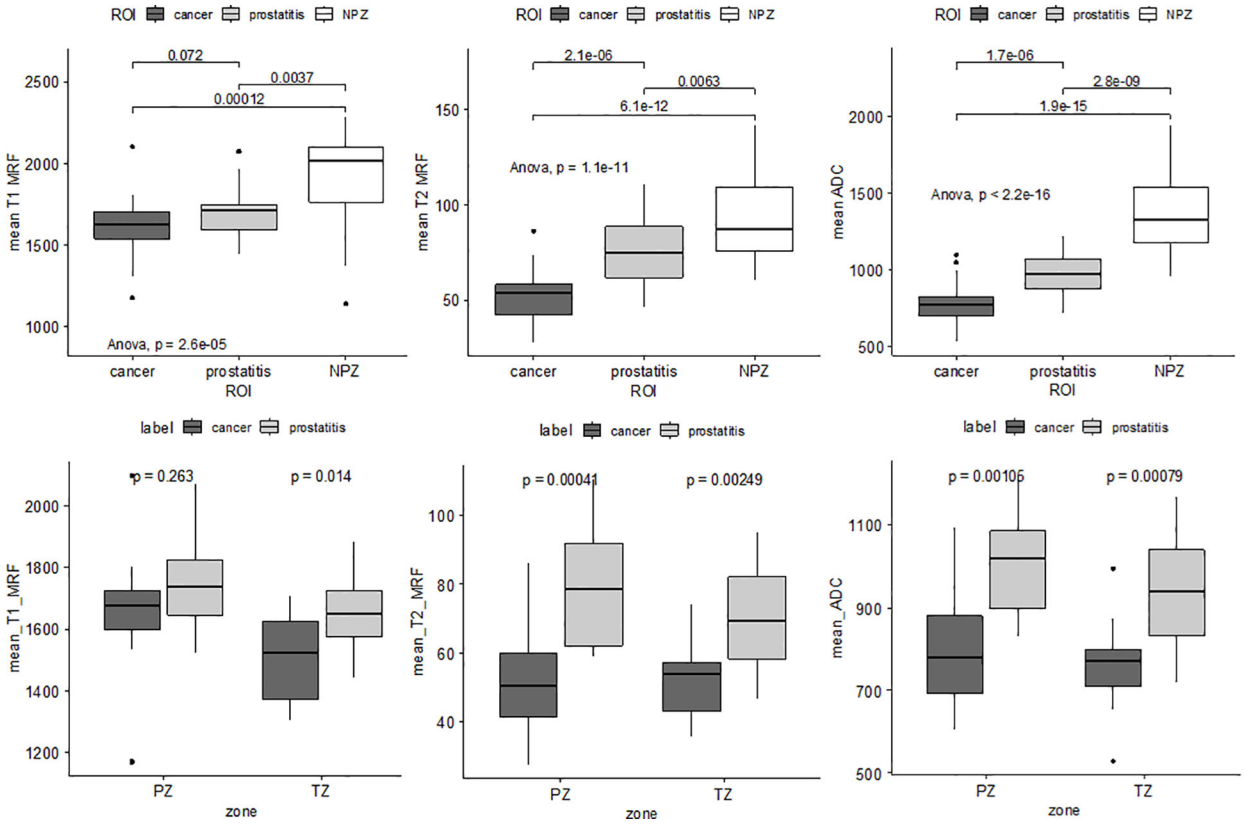

Figure 4:

Top row: Box plots illustrating statistically significant differences between prostate cancer prostatitis and normal peripheral zone (NPZ) in terms of mean T1, T2 MRF and ADC values, pair-wise along with ANOVA. Bottom row: Differences between prostate cancer and prostatitis in terms of mean T1, T2 MRF and ADC. T2 MRF and ADC show significant differences across peripheral (PZ) and transition zone (TZ) while T1 MRF is significantly different in the TZ, between prostate cancer and prostatitis.

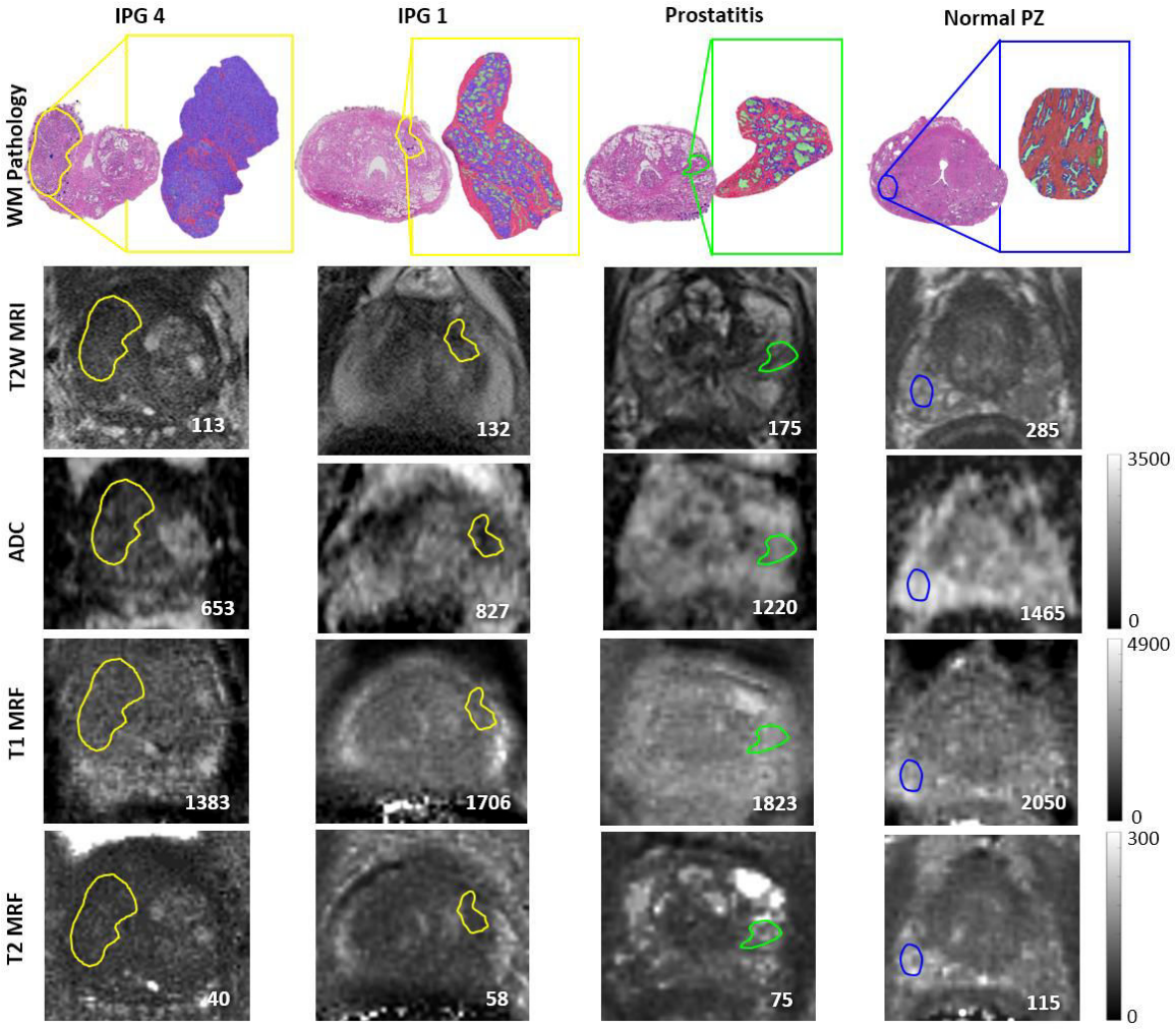

Figure 5:

Row 1: Tissue compartment segmentations on clinically significant (IPG >1), insignificant (IPG = 1), prostatitis and normal peripheral zone ROIs (purple epithelium, pink stroma and green lumen). Row 2,3: T2WI and ADC containing mapped ROIs from pathology. Row 4,5: T1, T2 MRF maps showing ROI mapped from T2WI. Mean values within the ROIs are provided in the lower right corner for each image.

Table 1:

Dataset Characteristics

Parameter	Value
# patients	14
Mean age (range) in years	62 (54–74)
Mean PSA (range) in ng/mL	9.4 (5.2–23.8)
# Prostate Cancer lesions	33
# in PZ,TZ	19, 14
ISUP Prognostic Group:	
1	15
2	9
3	4
4	4
5	1
# Prostatitis lesions	23
# in PZ,TZ	9, 14

PZ: Peripheral Zone; TZ: Transition Zone; PSA: Prostate Specific Antigen

Table 2:

Mean MRI (T2w, ADC), MRF (T1, T2), and Tissue Component Density Estimates within Prostate Cancer, Prostatitis and normal peripheral zone (PZ) ROIs; correlations with IPG

Parameter	Mean within ROIs						ANOVA	
	Prostate Cancer (PCa), N = 33			Correlation with IPGs	Prostatitis, N = 23	Normal PZ, IM = 24	F statistic	*p*-value
	IPG 1	IPG 2,3	IPG 4,5					
% Epithelium	0.32 ± 0.05	0.47 ± 0.12	0.69 ± 0.06	0.89*	0.35 ± 0.07	0.24 ± 0.09	35.1	<0.0001
% Lumen	0.17 ± 0.03	0.14 ± 0.04	0.08 ± 0.03	−0.71*	0.18 ± 0.05	0.20 ± 0.06	6.26	0.0002
% Stroma	0.48 ± 0.1	0.41± 0.1	0.22 ± 0.06	−0.73*	0.46 ± 0.07	0.56 ± 0.1	14.3	<0.0001
T2w	133 ± 23.4	129 ± 29.8	117 ± 11.52	−0.23	140 ± 37.6	217 ± 68	13.75	<0.0001
ADC	841 ± 112.4	758 ± 97.8	634 ± 61.1	−0.56	968 ± 133	1372 ± 233	47.37	<0.0001
T1 MRF	1643 ± 115	1568 ± 226	1528 ± 178	−0.34	1690 ± 154	1913 ± 350	6.36	0.0002
T2 MRF	54 ± 7.6	53 ± 15.3	38 ± 9.8	−0.39*	74 ± 17.6	95 ± 28	17.4	<0.0001

*Note: indicates statistical significance ($p < 0.05$)

Table 3:

Correlation coefficients between quantitative MR and tissue compartments of prostate cancer lesions and prostatitis within peripheral and transition zone

		Peripheral Zone (n_{PCa} = 19, n_P = 9)			Transition Zone (n_{PCa} = 14, n_P = 14)		
		%epithelium	%stroma	%lumen	%epithelium	%stroma	%lumen
Prostate Cancer	T1 MRF	−0.36	0.17	0.3	−0.56*	0.46*	0.42
	T2 MRF	−0.72*	0.52*	0.76*	0.1	−0.1	0.1
	ADC	−0.6*	0.63*	0.23	−0.28	−0.1	0.87*
Prostatitis	T1 MRF	0.3	−0.46	0.36	0.64*	−0.44	−0.5*
	T2 MRF	0.12	−0.45	0.54	−0.6*	0.56*	0.2
	ADC	0.05	0.08	−0.17	−0.4	0.19	0.5

*Indicates statistical significance ($p < 0.05$); PCa: Prostate Cancer; P: Prostatitis

Table 4:

Comparing correlations shown in previous works between T2w, ADC and tissue compartments on histopathology

	Our results	Kwak et. al.	Chatterjee et. al.*	Langer et. al. **
ADC – epithelium	−0.48	−0.56	−0.65	−0.50
ADC – lumen	0.37	0.47	0.68	0.57
ADC – stroma	0.37	0.30	0.35	0.13
T2WI – epithelium	−0.29	−0.39		
T2WI – lumen	0.40	0.36		
T2WI – stroma	0.16	0.18		

* − uses Spearman's rank correlation

** − uses mean slope